

# Nonlinear-optical spectral interferometry of nanostructures using coherent anti-Stokes Raman scattering

S.O. Konorov, V.P. Mitrokhin, I.V. Smirnova, A.B. Fedotov,  
D.A. Sidorov-Biryukov, A.M. Zheltikov

**Abstract.** The spectrum of coherent anti-Stokes Raman scattering (CARS) from Raman-active vibrations of gas-phase nitrogen molecules in a mesoporous silica aerogel host is experimentally studied. The CARS spectral profile under these conditions is a result of interference of the resonant part of nonlinear susceptibility, originating from nitrogen molecules in aerogel pores, and the nonresonant contribution, related to the mesoporous host. Raman-active modes of gas-phase molecular nitrogen give rise to intense resonances in the CARS spectrum, serving as reference spectral profiles for probing local parameters of a nanocomposite material (nanoCARS).

**Keywords:** coherent anti-Stokes Raman scattering, nanocomposite materials, nanooptics.

## 1. Introduction

Research into the inelastic, combinational scattering of light is one of the milestones in the history of physics at Moscow State University. This seminal work was done by L.I. Mandelstam and G.D. Landsberg, who observed the combinational scattering of light in crystalline quartz [1, 2] independently of experiments of C.V. Raman and K.S. Krishnan on inelastic scattering of light in liquids [3], later called the Raman effect. The discovery of stimulated [4–6] and coherent [7] regimes of Raman scattering gave rise to new methods of laser spectroscopy and time-resolved studies of ultrafast energy-transfer processes in molecular and atomic systems [8–12], stimulating the development of the quantum-control technique [13], laser cooling of atoms [14, 15], and efficient frequency conversion of laser radiation [12].

**S.O. Konorov, V.P. Mitrokhin, A.B. Fedotov, A.M. Zheltikov**  
Department of Physics, M.V. Lomonosov Moscow State University,  
Vorob'evy gory, 119992 Moscow, Russia;  
e-mail: zheltikov@phys.msu.ru;  
**I.V. Smirnova** Institut für Verfahrenstechnik, Technische Universität Berlin, Strasse des 17 Juni 135, 10623 Berlin, Germany;  
**A.B. Fedotov, D.A. Sidorov-Biryukov, A.M. Zheltikov** International Teaching and Research Laser Center, M.V. Lomonosov Moscow State University, Vorob'evy gory, 119992 Moscow, Russia

Received 6 August 2004  
Kvantovaya Elektronika 35 (1) 97–101 (2005)  
Translated by A.M. Zheltikov

Coherent anti-Stokes Raman scattering (CARS) [8–12] is one of the most widely used, efficient, and elegant methods in nonlinear spectroscopy. As a physical phenomenon, CARS was first observed and identified by P.D. Maker and R.W. Terhune [7] about 40 years ago. Researchers at Moscow State University, the founders of the Soviet–Russian school of nonlinear optics, have prominently contributed to the development of CARS [8]. In the early 1970s, S.A. Akhmanov supervised a group of researchers at the Department of Physics of Moscow State University, who pioneered in the development of CARS with frequency-tunable optical parametric oscillators [16]. This work demonstrated the unique potential of CARS and opened a new phase in laser spectroscopy. N.I. Koroteev and his colleagues have later developed a polarisation technique for coherent background suppression in CARS spectra [17, 18], allowing the sensitivity and selectivity of CARS spectroscopy to be substantially improved.

The up-to-date CARS technique [19, 20] can provide a high spatial, temporal, and spectral resolution in the diagnostics of excited gas media, plasmas, flames, and combustion. This method is extensively used for coherent microscopy of biological objects [21] and ionised spatially inhomogeneous gas media [22]. CARS renaissance of the past few years has been inspired by impressive achievements in femtosecond CARS [13], three-dimensional CARS microscopy [21], and coherence-controlled CARS [23]. Waveguide regimes of nonlinear-optical interactions [24], including waveguide CARS in hollow photonic-crystal fibres [25], provide a radical sensitivity improvement in CARS spectroscopy.

In this work, we demonstrate that the CARS technique is ideally suited for the metrology of nanocomposite materials and other objects of nano-optics. We will present the results of experimental studies of CARS spectra of Raman-active vibrations of gas-phase molecular nitrogen in a mesoporous silica aerogel host. The CARS spectral profile under these conditions is a result of interference of the resonant part of nonlinear susceptibility, originating from nitrogen molecules in aerogel pores, and the nonresonant contribution, related to the nanostructure. This spectral profile is shown to allow the probing of local parameters of nanostructures and nanocomposite materials (nanoCARS). On the eve of the historical 250th anniversary of Moscow State University, we are honored to contribute to this special issue, dedicating our work to the founders of the school of optical physics at Moscow University – pioneers of spectroscopy and nonlinear optics.

## 2. Theory of nanoCARS

Coherent anti-Stokes Raman scattering generally involves coherent excitation of Raman-active modes in a medium under study with a biharmonic pump field and probing of the thus phased Raman modes with an additional light field. The difference of frequencies  $\omega_1$  and  $\omega_2$  of the biharmonic pump field is scanned around the frequency of the Raman-active mode  $\omega_1 - \omega_2 \approx \Omega$  (the inset in Fig. 1), providing a high efficiency and a high selectivity of Raman-mode excitation. The third field with a frequency  $\omega_3$  is then applied to probe coherently excited Raman modes, giving rise to an anti-Stokes signal at the frequency  $\omega_a = \omega_1 - \omega_2 + \omega_3 = \omega_3 + \Omega$ , which is used to extract the spectroscopic information on the system. The CARS line profile is controlled by the interference of Raman-resonant and nonresonant parts of nonlinear-optical susceptibility,  $\chi_r^{(3)} = \chi_r^{(3)}(\omega_a; \omega_1, -\omega_2, \omega_3)$ , and  $\chi_{nr}^{(3)} = \chi_{nr}^{(3)}(\omega_a; \omega_1, -\omega_2, \omega_3)$ . In the scalar theory of CARS line profiles, the intensity of the CARS signal is represented as [8, 9]

$$I_a \propto |\chi_{nr}^{(3)} + \chi_r^{(3)}|^2 I_1 I_2 I_3, \quad (1)$$

where  $I_1$ ,  $I_2$ , and  $I_3$  are the intensities of the pump and probe fields.

The nonresonant coherent background, originating from the nonresonant nonlinear-optical susceptibility, often masks Raman resonances in CARS spectra, complicating CARS measurements and limiting the sensitivity of CARS spectroscopy. In certain situations, however, the nonresonant part can help to restore the phase information on the resonant part of  $\chi^{(3)}$  and to measure nonlinearities of optical materials [26, 27].

We now extend the scalar theory of CARS to the case of a nanocomposite material. Consider a nanocomposite system consisting of two components with dielectric constants  $\varepsilon_1$  and  $\varepsilon_2$  and cubic nonlinear-optical susceptibilities  $\chi_1^{(3)}$ ,  $\chi_2^{(3)}$ . The generic mixing rule for nonlinear susceptibilities is then written as [28, 29]

$$\chi_{eff}^{(3)} = \frac{1}{f_1} \left| \frac{\partial \varepsilon_{eff}}{\partial \varepsilon_1} \right| \left( \frac{\partial \varepsilon_{eff}}{\partial \varepsilon_1} \right) \chi_1^{(3)} + \frac{1}{f_2} \left| \frac{\partial \varepsilon_{eff}}{\partial \varepsilon_2} \right| \left( \frac{\partial \varepsilon_{eff}}{\partial \varepsilon_2} \right) \chi_2^{(3)}, \quad (2)$$

where  $f_1$  and  $f_2$  are the volume filling factors of the constituent materials. The effective dielectric constant of the nanocomposite material  $\varepsilon_{eff}$  is determined by the dielectric functions and the volume filling fractions of the constituent materials, as well as by the morphology of the nanocomposite. For nanocomposite materials with an architecture of a random network of pores, a good approximation for the effective dielectric constant is often provided by the Bruggeman formula [30],

$$f_1 \frac{\varepsilon_1 - \varepsilon_{eff}}{\varepsilon_1 + 2\varepsilon_{eff}} + f_2 \frac{\varepsilon_2 - \varepsilon_{eff}}{\varepsilon_2 + 2\varepsilon_{eff}} = 0. \quad (3)$$

The generic idea of nanoCARS is to use a reference CARS line profile (such profiles have been accurately measured for a broad class of Raman-active molecular vibrations) as a local probe for the parameters of a nanocomposite material. The second material in a nanocomposite structure provides a nonresonant contribution to

the mixing rule, thus deforming the reference CARS line profile. We will analyse in greater detail a Raman resonance with a Lorentzian profile:

$$\chi_1^{(3)} = -\frac{\bar{\chi}^{(3)}}{i + \Delta}, \quad (4)$$

where  $\Delta = (\omega_1 - \omega_2 - \Omega)/\Gamma$  is the frequency detuning of the biharmonic pump  $\omega_1 - \omega_2$  from the frequency  $\Omega$  of the Raman-active mode normalised to the linewidth  $\Gamma$ . In view of Eqns (1)–(4), the scalar-theory expression for the intensity of the CARS signal from an isotropic nanocomposite material is written as

$$I_a \propto \left| \frac{1}{f_1} \left| \frac{\partial \varepsilon_{eff}}{\partial \varepsilon_1} \right| \left( \frac{\partial \varepsilon_{eff}}{\partial \varepsilon_1} \right) \frac{\bar{\chi}^{(3)} \Delta}{1 + \Delta^2} \right. \\ \left. - \frac{1}{f_2} \left| \frac{\partial \varepsilon_{eff}}{\partial \varepsilon_2} \right| \left( \frac{\partial \varepsilon_{eff}}{\partial \varepsilon_2} \right) \chi_2^{(3)} \right|^2 + \left| \frac{1}{f_1} \left( \frac{\partial \varepsilon_{eff}}{\partial \varepsilon_1} \right)^2 \frac{\bar{\chi}^{(3)}}{1 + \Delta^2} \right|^2. \quad (5)$$

As can be seen from Eqn (5), the nanostructured host distorts the reference CARS profile (Fig. 1). Accurately pre-calibrated CARS profiles can therefore be used to measure local parameters of nanocomposite materials.

## 3. Experimental

Our experiments were performed with mesoporous silica dioxide used as a nanocomposite system. The synthesis of aerogels was based on the hydrolysis of metal alkoxide [31, 32]. The hydrolysed metal alkoxide undergoes a condensation reaction, forming a metal oxide gel, from which solvents are supercritically extracted to form an aerogel. Unique properties of aerogels for nonlinear optics originate from their low density ( $0.003\text{--}0.15\text{ g cm}^{-3}$ ) and a high porosity (90 %–99 %). An open structure of pores in

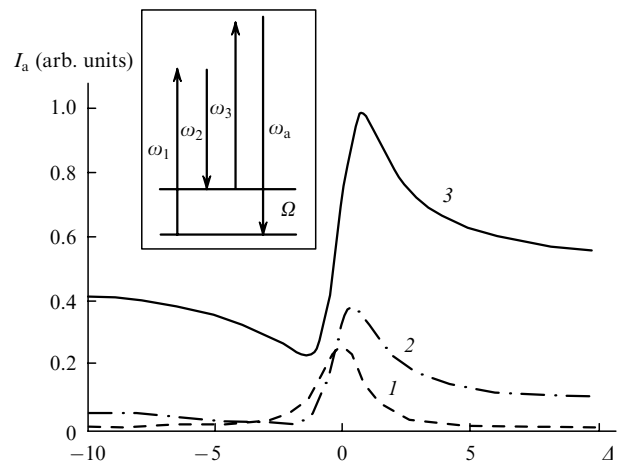


**Figure 1.** Intensity of the CARS signal from a binary nanocomposite consisting of materials with dielectric constants  $\varepsilon_1 = 1$  and  $\varepsilon_2 = 2.25$ , the volume filling fractions  $f_1$ , and  $f_2 = 1 - f_1$ , and third-order nonlinear susceptibilities  $\chi_1^{(3)} = -\bar{\chi}^{(3)}/(i + \Delta)$  and  $\chi_2^{(3)}$  calculated as a function of the normalised frequency detuning from the Raman resonance  $\Delta = (\omega_1 - \omega_2 - \Omega)/\Gamma$  for  $|\bar{\chi}^{(3)}|/|\chi_2^{(3)}| = 0.01$ ,  $f_2 = 0$  (curve 1), 0.02 (2), and 0.05 (3). The inset shows the diagram of the CARS process.

aerogels is ideally suitable for the creation of high-porosity hosts for materials with high nonlinearities, as well as for the development of sensors based on laser spectroscopy.

We performed two-colour CARS spectroscopy ( $\omega_1 = \omega_3, \omega_a = 2\omega_1 - \omega_2$ ) of Raman-active vibrations of nitrogen and toluene molecules in a mesoporous silica aerogel host with a typical pore size of 8–15 nm and a porosity of 97%–98%. The content of nitrogen molecules in aerogel pores corresponded to the natural content of molecular nitrogen in the atmospheric air under normal conditions. Toluene molecules were infiltrated into aerogels in the gas phase by placing samples on top of a cell containing toluene solution.

The laser system employed in our experiments (Fig. 2) was based on a *Q*-switched Nd : YAG master oscillator, which generated 15-ns pulses of 1.064- $\mu\text{m}$  radiation. These pulses were then amplified and converted into the second harmonic with a KDP crystal. The second harmonic produced in this crystal served as one of the pump beams in the CARS process (frequency  $\omega_1$ ). Frequency-tunable radiation of a sulforhodamine 101 dye laser (DL in Fig. 2) served as the second pump beam in the CARS process (frequency  $\omega_2$ ). Glan prisms and polarisation plates were employed to rotate polarisations of the second-harmonic and dye-laser pump fields. A Glan prism placed behind the nanocomposite sample served to analyse polarisation of the CARS signal. A dichroic mirror was used to couple the spherically focused pump laser beams into a silica aerogel sample. The energies of pump fields with frequencies  $\omega_1$  and  $\omega_2$  were varied within the ranges of 10–200  $\mu\text{J}$  (second-harmonic radiation) and 10–80  $\mu\text{J}$  (dye-laser radiation), respectively.

The frequency difference  $\omega_1 - \omega_2$  was scanned through the frequencies of 2331- $\text{cm}^{-1}$  vibrations of nitrogen molecules and 1004- $\text{cm}^{-1}$  vibrations of toluene. The CARS signal, generated at the frequency  $\omega_{\text{CARS}} = 2\omega_1 - \omega_2$  through Raman-active vibrations of molecular nitrogen or toluene (the inset in Fig. 1), was collimated with a spherical lens, separated from the pump and probe beams with a set of optical filters, dispersed with a monochromator, and detected with a photomultiplier (Fig. 2).

## 4. Results and discussion

Even on Raman resonance, the cubic nonlinear optical susceptibility related to vibrations of gas-phase molecular nitrogen in the atmospheric air filling the pores of silica aerogel is much lower than the nonresonant contribution related to the solid-state nanostructured host,  $|\bar{\chi}^{(3)}|/|\chi_2^{(3)}| \ll 1$ . Still, due to the high porosity of the host, Raman-resonant vibrations of gas-phase molecular nitrogen give rise to an easily detectable CARS signal with a wavelength of 473 nm, allowing the spectral analysis of this signal (Fig. 3). To visualise the contribution of the mesoporous host, we compared the profiles of the 2331- $\text{cm}^{-1}$  resonance in CARS spectra related to molecular nitrogen in free atmospheric-pressure air [dashed line (1) in Fig. 3] and in silica aerogel [dots connected with line (2), serving as a guide for the eye in Fig. 3]. This comparison shows that the high-porosity host distorts the CARS spectral profile.

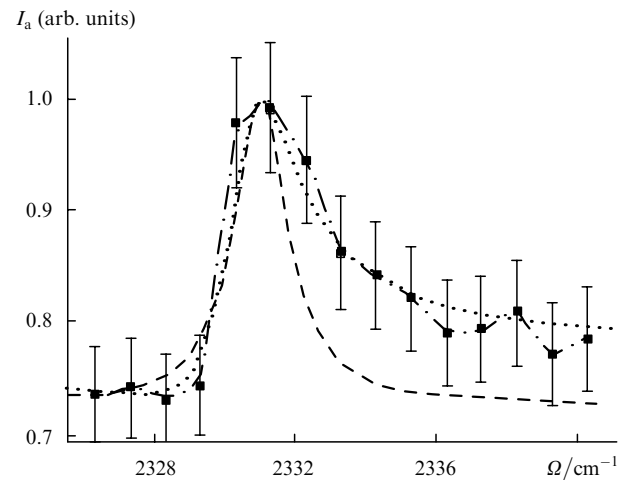


**Figure 3.** Spectrum of the CARS signal from 2331- $\text{cm}^{-1}$  Raman-active vibrations of molecular nitrogen in free atmospheric-pressure air [line (1)] and in the atmospheric air filling the pores of the silica aerogel host under normal conditions [dots connected with line (2)]. Dotted line (3) shows the theoretical fit of the experimental data with  $|\bar{\chi}_{N_2}^{(3)}|/|\chi_{\text{aerogel}}^{(3)}| = 0.002$  for the polarisation arrangement implemented in experiments.

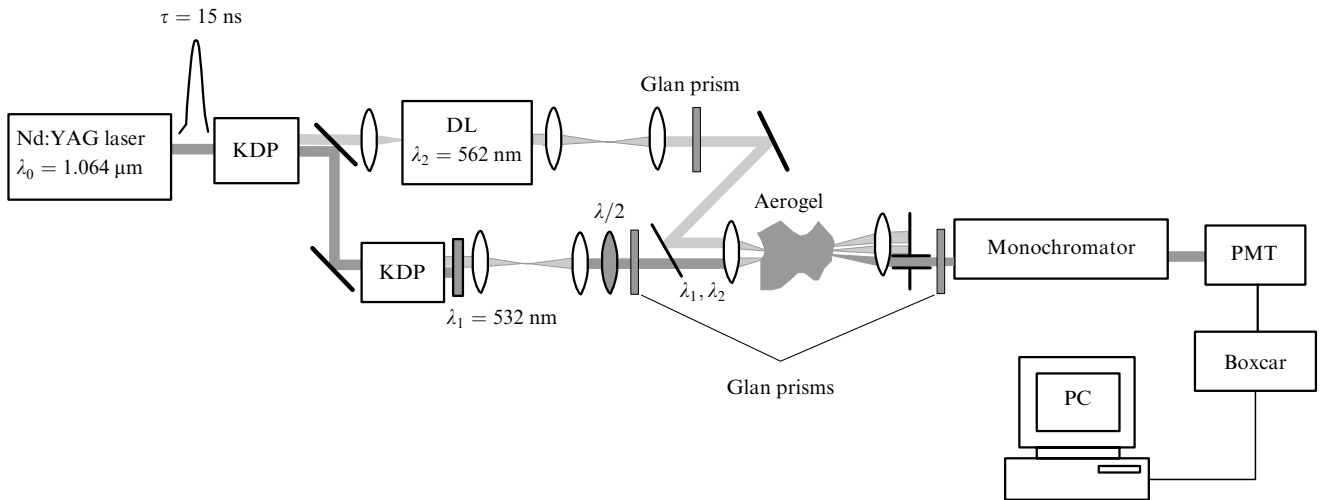


**Figure 2.** Scheme of the experimental setup for nanoCARS spectroscopy of nanocomposite materials based on aerogels.

Dotted line (3) in Fig. 3 displays the fit of the experimental data using Eqn (5) with  $|\bar{\chi}_{N_2}^{(3)}|/|\chi_{\text{aerogel}}^{(3)}| = 0.002$ , typical of the studied nanocomposite and the employed polarisation CARS arrangement. Overall, the theoretical fit reproduces the experimental CARS spectral profile with a reasonable accuracy. Deviations of the experimental spectral profiles from the fit in Fig. 3 can be partially attributed to the non-Lorentzian shape of the Raman line of molecular nitrogen probed in our experiments (see, e.g., [33]). The qualitative agreement between the experimental data and theoretical fit indicates the applicability of effective-medium models for the description of CARS spectra of Raman-active molecular vibrations in the gas phase infiltrating mesopores of aerogels.

Figure 4 presents CARS spectra of toluene molecules from a standard cell (the dashed curve) and a mesoporous aerogel host (dots). These spectra demonstrate a drastic change in CARS spectral profiles as the regime with a high ratio  $|\bar{\chi}^{(3)}|/|\chi_{\text{nr}}^{(3)}| \gg 1$ , characteristic of toluene solution in a standard cell, is replaced by the regime of nanoCARS with a low concentration of Raman-active species. The sensitivity of the CARS spectral profile to the ratio of the resonant part of nonlinear-optical susceptibility, associated in this case with toluene molecules, to the nonresonant part of  $\chi^{(3)}$  suggests the possibility of using the CARS technique to measure the local parameters of nanocomposite materials, including the porosity and the effective refractive index. The local-field enhancement of the pump field in the pores [29] can, on the other hand, substantially increase the resonant component of the CARS signal (see also [34]). This effect can be employed for the creation of efficient sensors, as well as optical modulators and switches based on high-porosity aerogel-architecture nanocomposite materials.

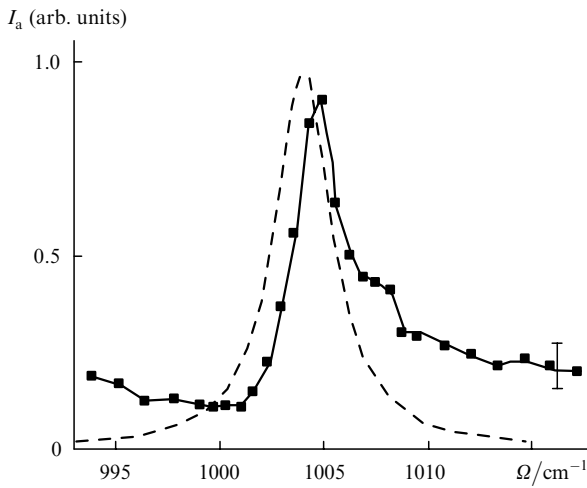


**Figure 4.** Spectrum of the CARS signal from Raman-active vibrations of toluene in a standard cell (dashed line) and in a silica aerogel sample infiltrated with toluene vapour (dots).

## 5. Conclusions

Experimental and theoretical studies of CARS from Raman-active vibrations of gas-phase nitrogen molecules in a mesoporous silica aerogel host reveal a high potential of the CARS technique for the metrology of nanocomposite materials and other systems of nano-optics. The CARS

spectral profile under these conditions is a result of interference of the resonant part of nonlinear susceptibility, originating from nitrogen molecules in aerogel pores, and the nonresonant contribution, related to the mesoporous host. Raman-active modes of gas-phase molecular nitrogen give rise to intense resonances in the CARS spectrum, serving as reference spectral profiles for probing local parameters of a nanocomposite material, such as the porosity and the effective refractive index.

**Acknowledgements.** Fruitful discussions with P.K. Kashkarov, L.A. Golovan', and S.V. Zabotnov are gratefully acknowledged. This study was supported in part by the President of Russian Federation Grant MD-42.2003.02, the Russian Foundation for Basic Research (Project Nos 03-02-16929, 03-02-20002-BNTs, 04-02-39002-GFEN2004, and 04-02-81036-Bel2004), and INTAS (Project Nos 03-51-5037 and 03-51-5288). The research described in this publication was made possible in part by Award No. RP2-2558 of the U.S. Civilian Research & Development Foundation (CRDF) for the Independent States of the Former Soviet Union. This material is also based upon work supported by the European Research Office of the US Army under Contract No. 62558-04-P-6043.

## References

1. Mandelstam L.I., Landsberg G.S. *Zh. Ross. Fiz. Khim. Obshch.*, **60**, 335 (1928).
2. Landsberg G., Mandelstam L. *Naturwissenschaften*, **16**, 557 (1928).
3. Raman C.V., Krishnan K.S. *Nature*, **121**, 501 (1928).
4. Woodbury E.J., Ng W.K. *Proc. IRE*, **50**, 2347 (1962).
5. Hellwarth R.W. *Phys. Rev.*, **130**, 1850 (1963).
6. Garmire E., Pandarese E., Townes C.H. *Phys. Rev. Lett.*, **11**, 160 (1963).
7. Maker P.D., Terhune R.W. *Phys. Rev. A*, **137**, 801 (1965).
8. Akhmanov S.A., Koroteev N.I. *Metody nelineinoi optiki v spektroskopii rasseyaniya sveta* (Methods of Nonlinear Optics in Light Scattering Spectroscopy) (Moscow: Nauka, 1981).
9. Eesley G.L. *Coherent Raman Spectroscopy* (Oxford: Pergamon, 1981).
10. Druet S.A.J., Taran J.-P.E. *Prog. Quantum Electron.*, **7**, 1 (1981).
11. Eckbreth A.C. *Laser Diagnostics for Combustion Temperature and Species* (Cambridge, MA: Abacus, 1988).
12. Zheltikov A.M., Koroteev N.I. *Usp. Fiz. Nauk*, **169**, 385 (1999) [*Phys. Usp.*, **42**, 321 (1999)].
13. Kiefer W. (Ed.) *Femtosecond Coherent Raman Spectroscopy. Spec. Issue J. Raman Spectrosc.*, **31** (1/2) (2000).
14. Heinzen D.J., Wineland D.J. *Phys. Rev. A*, **42**, 2977 (1990).
15. Monroe C., Meekhof D.M., King B.E., Jefferts S.R., Itano W.M., Wineland D.J., Gould P. *Phys. Rev. Lett.*, **75**, 4011 (1995).
16. Akhmanov S.A., Dmitriev V.G., Kovrigin A.I., Koroteev N.I., Tunkin V.G., Kholodnykh A.I. *Pis'ma Zh. Eksp. Teor. Fiz.*, **15**, 600 (1972) [*JETP Lett.*, **15**, 425 (1972)].
17. Koroteev N.I., Endemann M., Byer R.L. *Phys. Rev. Lett.*, **43**, 398 (1979).
18. Aslanyan L.S., Bunkin A.F., Koroteev N.I. *Opt. Spektrosk.*, **46**, 165 (1979).
19. Radi P., Zheltikov A.M. (Eds) *Nonlinear Raman Spectroscopy. Spec. Issue J. Raman Spectrosc.*, **33** (11/12) (2002).
20. Radi P., Zheltikov A.M. (Eds) *Nonlinear Raman Spectroscopy II. Spec. Issue J. Raman Spectrosc.*, **34**, (12) (2003).
21. Zumbusch A., Holtom G.R., Sunney Xie X. *Phys. Rev. Lett.*, **82**, 4142 (1999).
22. Akimov D.A., Konorov S.O., Sidorov-Biryukov D.A., Naumov A.N., Fedotov A.B., Zheltikov A.M. *Proc. SPIE Int. Soc. Opt. Eng.*, **4749**, 101 (2002).
23. Dudovich N., Oron D., Silberberg Y. *Nature*, **418**, 512 (2002).

- 
- doi> 24. Zheltikov A.M. *Usp. Fiz. Nauk*, **172**, 743 (2002) [*Phys. Usp.*, **45**, 687 (2002)].
  - doi> 25. Konorov S.O., Sidorov-Biryukov D.A., Bugar I., Chorvat D. Jr., Chorvat D., Serebryannikov E.E., Bloember M.J., Scalora M., Miles R.B., Zheltikov A.M. *Phys. Rev. A*, **70**, 023807 (2004).
  - doi> 26. Levenson M.D., Flytzanis C., Bloembergen N. *Phys. Rev. B*, **6**, 3962 (1972).
  - doi> 27. Levenson M.D., Bloembergen N. *Phys. Rev. B*, **10**, 4447 (1974).
  - doi> 28. Zeng X.C., Bergman D.J., Hui P.M., Stroud D. *Phys. Rev. B*, **38**, 10970 (1988).
  - doi> 29. Sipe J.E., Boyd R.W. *Phys. Rev. A*, **46**, 1614 (1992).
  - 30. Bruggeman D.A.G. *Ann. Phys.*, **24**, 636 (1935).
  - 31. Fricke J. (Ed.) *Aerogels* (Berlin: Springer, 1986).
  - doi> 32. Smirnova I., Arlt W. *J. Sol-Gel Science Technol.*, **28**, 175 (2003).
  - doi> 33. Dreier T., Schüller G., Suvernev A.A. *J. Chem. Phys.*, **100**, 6275 (1994).
  - 34. Zheltikov A.M. *J. Opt. Soc. Am. B*, in press.